Supporting Information

for

Mechanistic insights into electrochemical nitrate reduction over *d*- and *p*-block Cu-based single-atom alloy catalysts: A DFT study

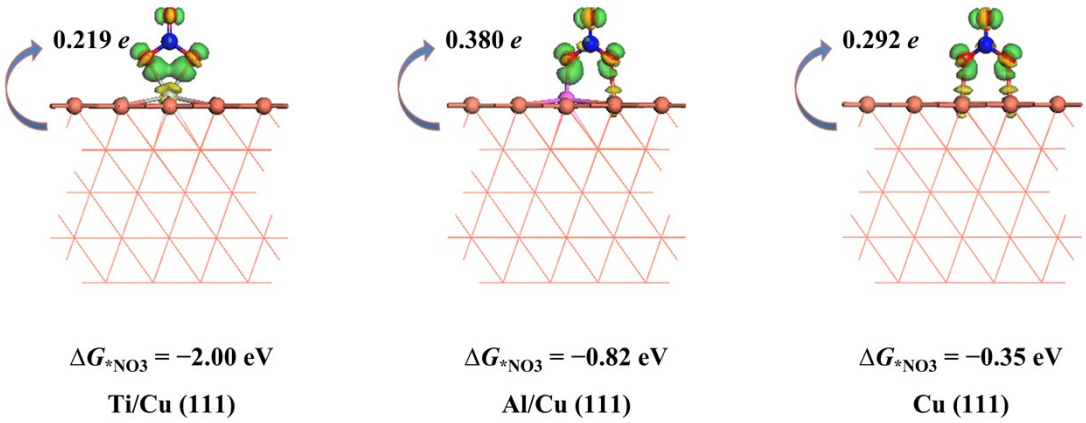

Fig. S1 Adsorption configurations of NO_3^- on Ti/Cu (111), Al/Cu (111), and Cu (111). Yellow and green regions indicate electron depletion and accumulation.

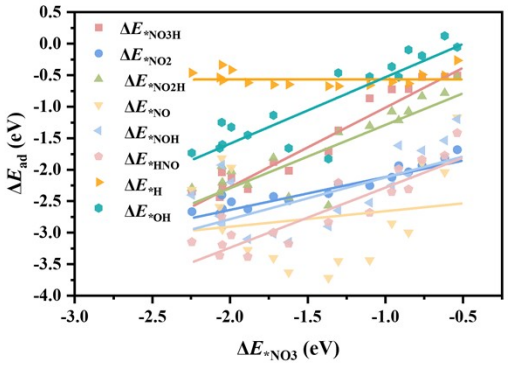

Intermediates	Fitting equation	R^2
ΔE_{*NO3H}	y = 1.26x + 0.25	0.95
ΔE_{*NO2}	y = 0.52x − 1.59	0.91
ΔE_{*NO2H}	y = 1.00x − 0.29	0.76
ΔE_{*NO}	y = 0.25x − 2.41	0.03
ΔE_{*NOH}	y = 0.66x − 1.45	0.37
ΔE_{*HNO}	y = 0.95x − 1.33	0.80
ΔE_{*H}	y = 0.00x − 0.56	0.00
ΔE_{*OH}	y = 1.05x + 0.52	0.79

Fig. S2 Relationships between the ΔE_{ad} of NO_3RR intermediates and ΔE_{*NO3} on SAAs.

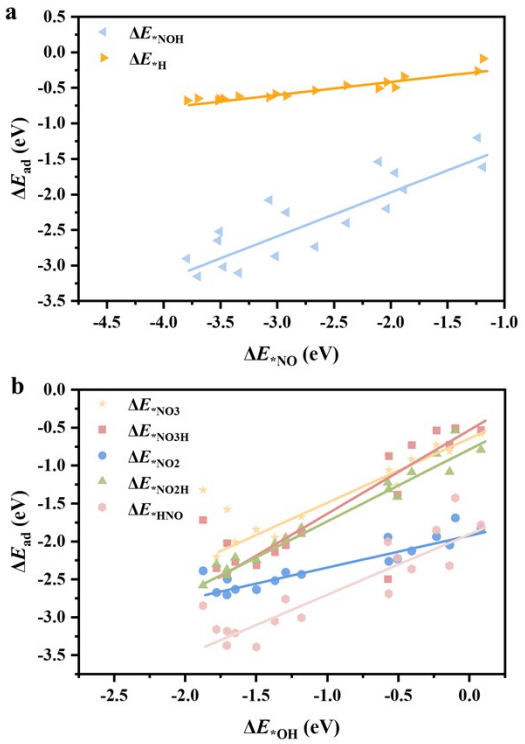

Intermediates	Fitting equation	R^2
ΔE_{*NOH}	y = 0.62x − 0.73	0.74
ΔE_{*H}	y = 0.18x − 0.05	0.86

Intermediates	Fitting equation	R^2
ΔE_{*NO3}	y = 0.85x − 0.61	0.90
ΔE_{*NO3H}	y = 1.10x − 0.53	0.94
ΔE_{*NO2}	y = 0.42x − 1.92	0.82
ΔE_{*NO2H}	y = 0.95x − 0.79	0.96
ΔE_{*HNO}	y = 0.80x − 1.91	0.79

Fig. S3 Relationships between ΔE_{ad} of NO_3RR intermediates and ΔE_{*NO} (a) and ΔE_{*OH} (b) on SAAs.

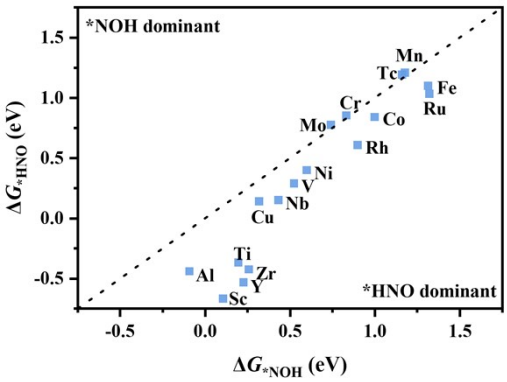

Fig. S4 Comparison of $\Delta G_{*\mathrm{NOH}}$ and $\Delta G_{*\mathrm{HNO}}$ on SAAs.

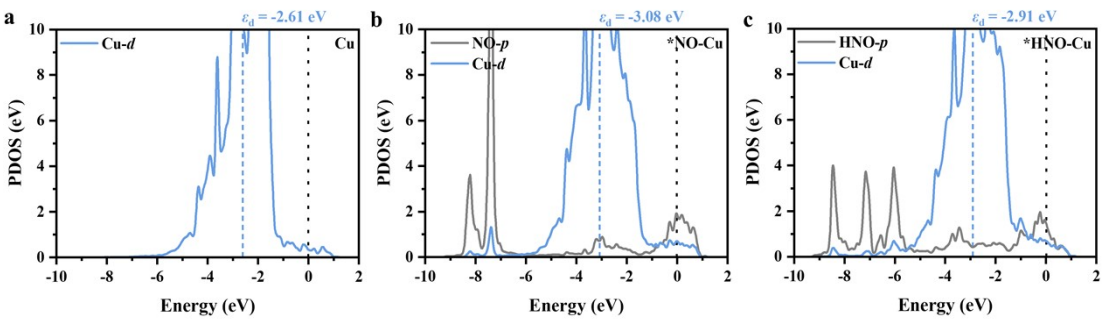

Fig. S5 (a) PDOS of Cu (111). (b and c) PDOS of adsorbed *NO and *HNO on Cu (111). Blue dashed lines mark the Cu-*d* band center.

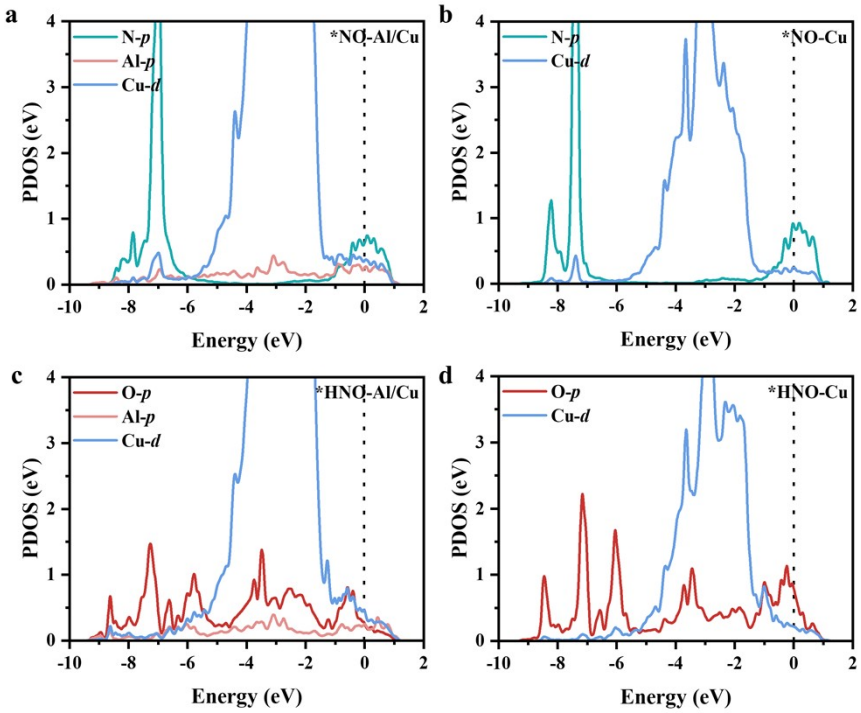

Fig. S6 PDOS of N-*p* in *NO (a and b) and O-*p* in *HNO (c and d) on Al/Cu (111) and Cu (111).

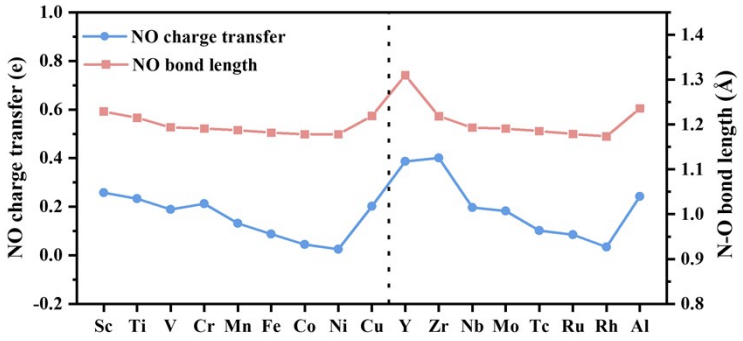

Fig. S7 The number of electrons transferred from the catalyst surface to *NO and the N-O bond length.

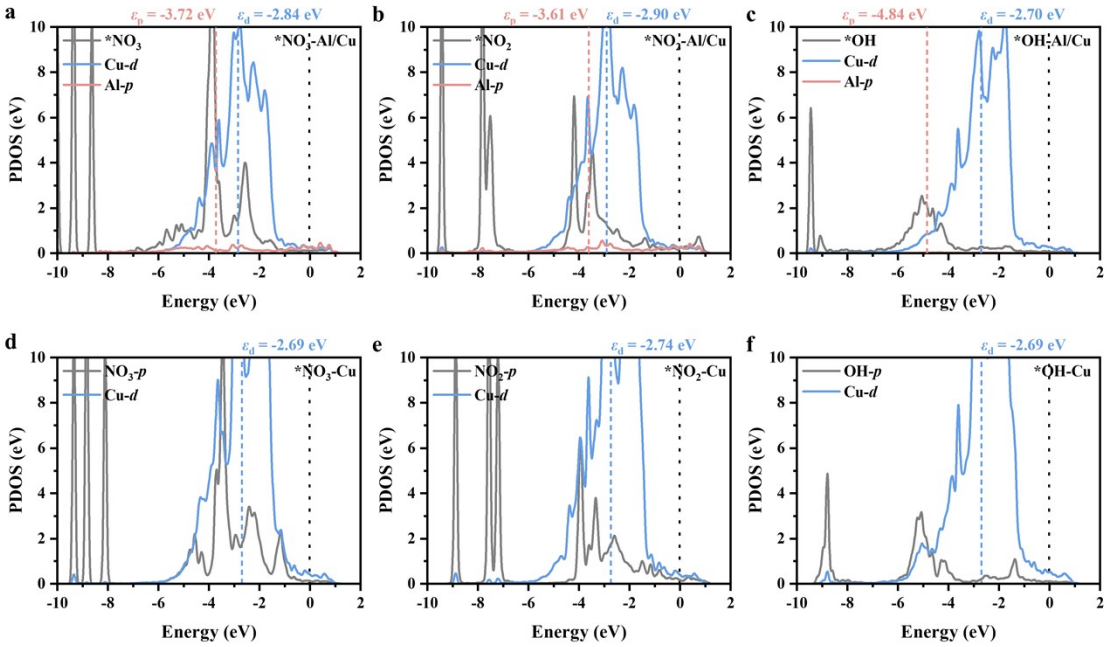

Fig. S8 PDOS of adsorbed *NO_3 (a), *NO_2 (b), and *OH (c) on Al/Cu (111). PDOS of adsorbed *NO_3 (d), *NO_2 (e), and *OH (f) on Cu (111). Pink and blue dashed lines mark the Al-p and Cu-d band centers.

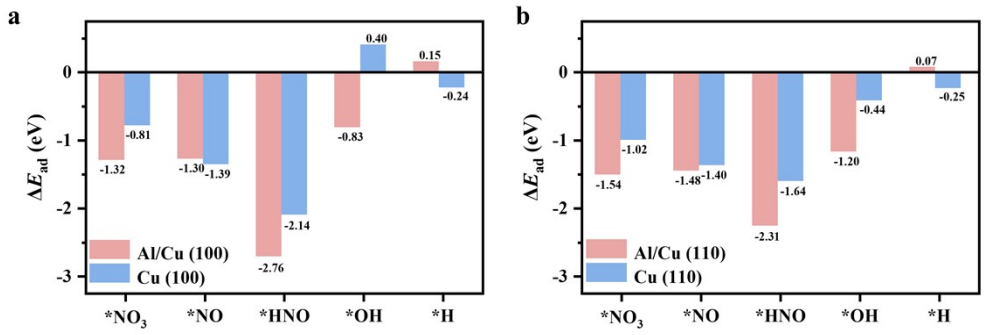

Fig. S9 ΔE_{ad} of NO_3^-, NO, HNO, OH, and H on Al/Cu (100) and Cu (100) (a), and Al/Cu (110) and Cu (110) (b).

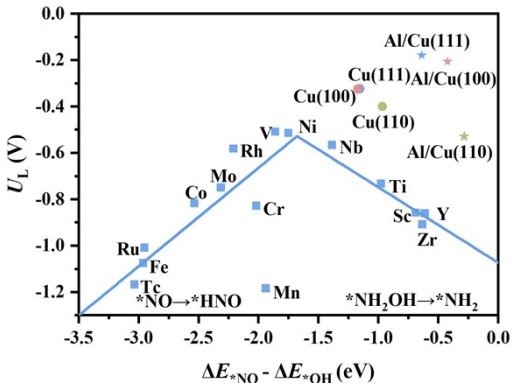

Fig. S10 Facet-dependent positions of Cu (100), Al/Cu (100), Cu (110), and Al/Cu (110) on the NO_3RR volcano plot constructed with the descriptor $\Delta E_{*NO} - \Delta E_{*OH}$.

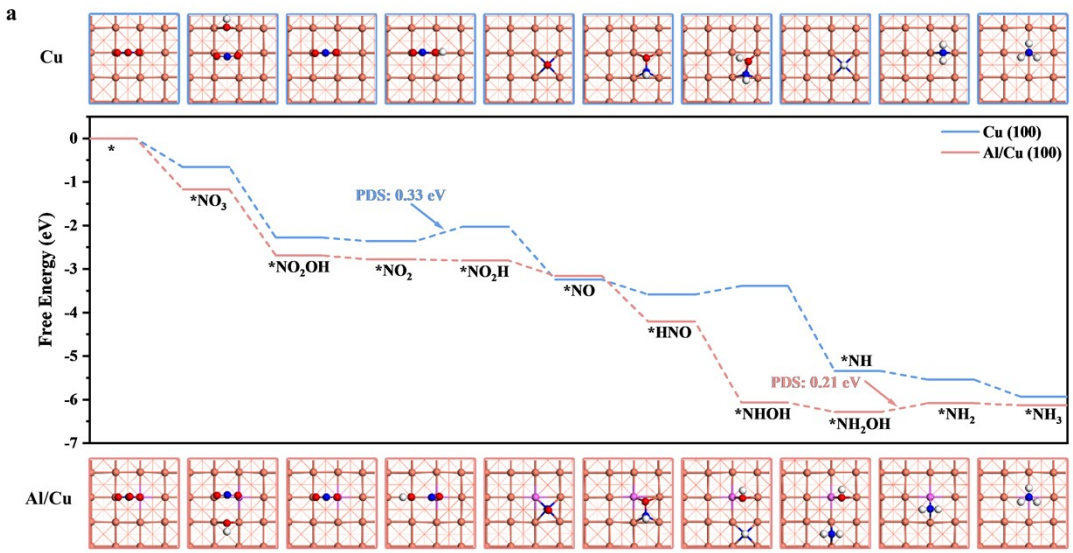

Fig. S11 Δ*G* diagrams and corresponding reaction intermediates during NO_3RR on Cu (100) and Al/Cu (100).

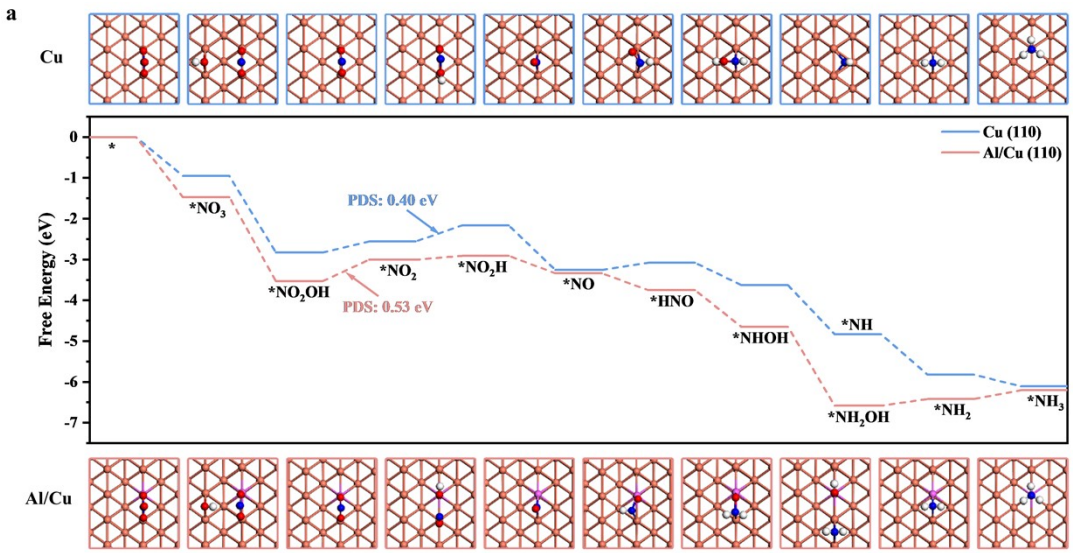

Fig. S12 Δ*G* diagrams and corresponding reaction intermediates during NO_3RR on Cu (110) and Al/Cu (110).

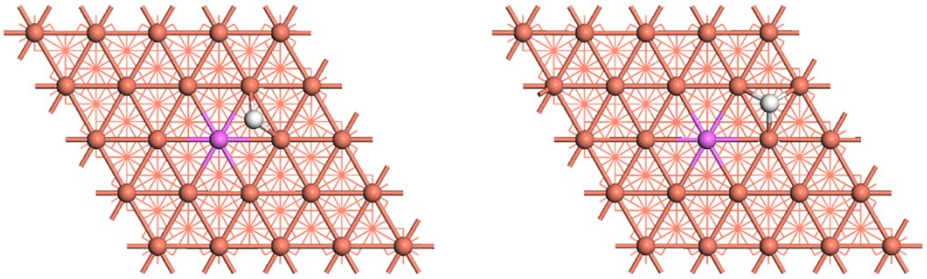

Fig. S13 H adsorption configurations at Al site (left) and Cu site (right) on Al/Cu (111).

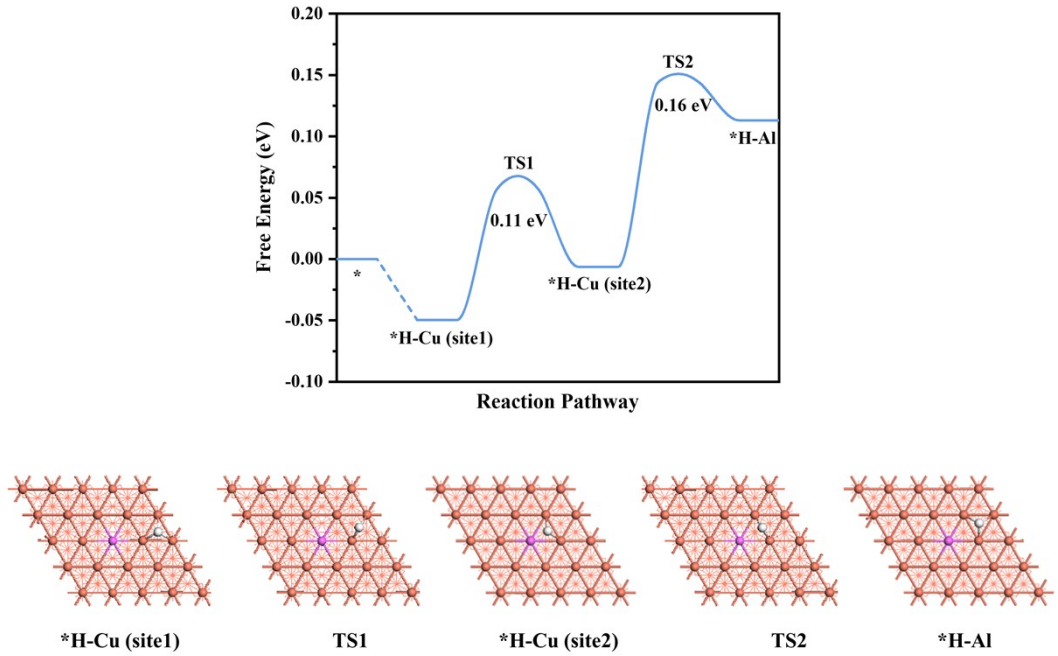

Fig. S14 Δ*G* diagrams and corresponding reaction intermediates during H spillover on Al/Cu (111).

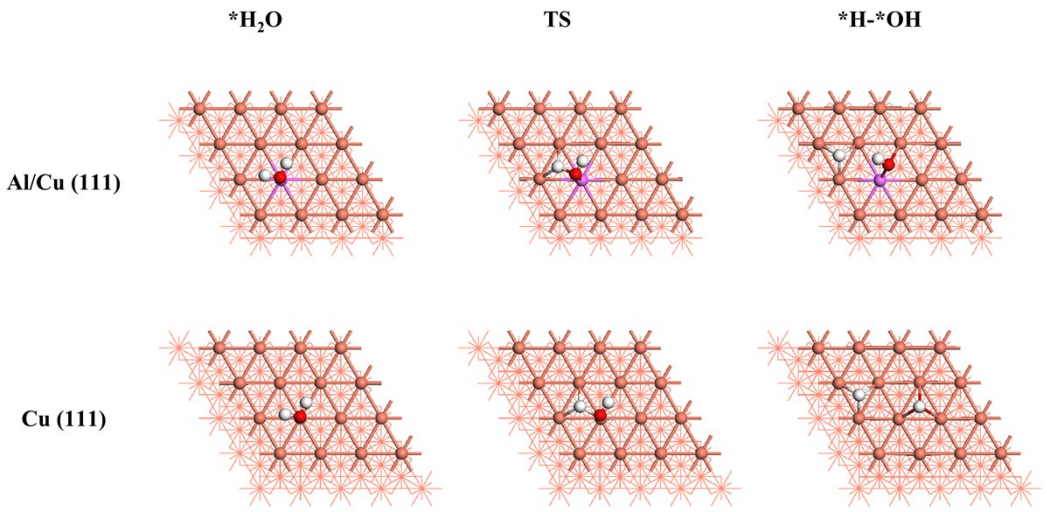

Fig. S15 The corresponding reaction intermediates of H_2O dissociation on Al/Cu (111) and Cu (111).